Science Bulletin 67 (2022) 1954–1957

Contents lists available at ScienceDirect

Science Bulletin

journal homepage: www.elsevier.com/locate/scib

Short Communication

Two-dimensional Dirac-line semimetals resistant to strong spin–orbit coupling

Deping Guo [a,1], Pengjie Guo [a,b,f,1], Shijing Tan [c], Min Feng [d,e], Limin Cao [d], Zheng-Xin Liu [a,*], Kai Liu [a,*], Zhong-Yi Lu [a], Wei Ji [a,*]

[a] Beijing Key Laboratory of Optoelectronic Functional Materials & Micro-Nano Devices, Department of Physics, Renmin University of China, Beijing 100872, China
[b] Songshan Lake Materials Laboratory, Dongguan 523808, China
[c] Hefei National Laboratory for Physical Sciences at the Microscale, University of Science and Technology of China, Hefei 230026, China
[d] School of Physics and Technology and Key Laboratory of Artificial Micro- and Nano-Structures of Ministry of Education, Wuhan University, Wuhan 430072, China
[e] Institute for Advanced Studies, Wuhan University, Wuhan 430072, China
[f] Beijing National Laboratory for Condensed Matter Physics, Institute of Physics, Chinese Academy of Sciences, Beijing 100190, China

ARTICLE INFO

Article history:
Received 12 June 2022
Received in revised form 1 August 2022
Accepted 5 September 2022
Available online 6 September 2022

Topological materials have attracted extensive attention in condensed matter physics because of their exotic physical properties and promising potential applications. If the bulk gap of an insulator closes at certain nodal points or lines in the Brillouin zone (BZ), the resultant gapless phase is known as the topological semimetal (TSM) [1]. Dirac nodal line semimetals (DNLSMs) [2,3] have been sought as novel quantum materials presenting quantum anomalies [4,5]. The DNLSMs against spin-orbit coupling (SOC) were discovered in several three-dimensional (3D) bulk materials [6–8]. Flourishing two-dimensional (2D) van der Waals (vdW) materials are, in comparison with their 3D counterparts, easier to experimentally measure and manipulate. However, 2D materials have one less dimension of translation symmetry operation, and the corresponding symmetry operations and groups are significantly reduced, narrowing the range of candidate structures. In some 2D materials, the non-symmorphic symmetry [9] is shown to protect the fourfold degeneracy of DPs at certain isolated k points against SOC [10–12], but no SOC resistant fourfold DNL state was even predicted in real materials so far.

Here, we found that a specific $\mathscr{C}_{2v} \times Z_2^T$ nonsymmorphic point group (where Z_2^T is the joint space-inversion and time-reversal symmetry) is the particular symmetry in 2D crystal structures that guarantees a stable fourfold-degenerate DNLSM. This intrinsic 2D DNLMS is resistant to SOC and is realized in a novel allotrope, i.e., the brick phase (Fig. 1a–c), of group-VA elemental layers, among which a three-atomic-layer (3-AL) bismuth (Bi) thin film was used as a prototype. Its valence electron occupation guarantees that the DNLSM state is near the Fermi level. This exotic electronic structure hosts a nearly "neat" DNLSM state. We also found the DNLSM state in phosphorous (P), arsenic (As), and antimony (Sb) thin films. These 2D thin films are expected to substantially promote the development and the exploration of 2D DNLSMs with exotic quantum phases and properties.

Fig. 1b shows the side view of a 3-AL Bi film and the stacked structure of a brick wall is more clearly illustrated in Fig. 1c, hence the name of the phase. Its lattice constants a and b are 4.85 and 4.53 Å, respectively. In each AL, the Bi atoms form flat zigzag chains oriented along the y-axis (Fig. 1a). The total energy of the brick phase is at least 40 meV/atom lower than other 3-AL configurations (Fig. S1 online).

The symmetry of the brick phase is described by the nonsymmorphic layer group pmma (No. 41), whose point group $G = D_{2h} \times Z_2^T$ is generated by C_{2x}, C_{2y}, M_z, and $\widetilde{T}$ ($\widetilde{T}$ = **IT**). Since the spectrum degeneracy at the boundary of the Brillouin zone is protected by the irreducible projective representation (Rep) of the corresponding little co-group, a SOC resistant Dirac nodal line on the BZ boundary needs the protection of a consistent nontrivial little co-group (a subgroup of $D_{2h} \times Z_2^T$). The $\mathscr{C}_{2v} \times Z_2^T$ group was found to be the certain little co-group symmetry in 2D satisfying the requirements of the robust fourfold degeneracy on the nodal line, which could be understood in two folds. Firstly, the spin-½ Kramers degeneracy is protected by $\widetilde{T}^2 = -1$, or by the anti-commutation relation between symmetry operations $\{C_{2x}|\ (0, ½, 0)\}$ and $\{M_y|\ (0, ½, 0)\}$. Secondly, the orbital degeneracy lies in that

* Corresponding authors.
E-mail addresses: liuzxphys@ruc.edu.cn (Z.-X. Liu), kliu@ruc.edu.cn (K. Liu), wji@ruc.edu.cn (W. Ji).
[1] These authors contributed equally to this work.

https://doi.org/10.1016/j.scib.2022.09.008
2095-9273/

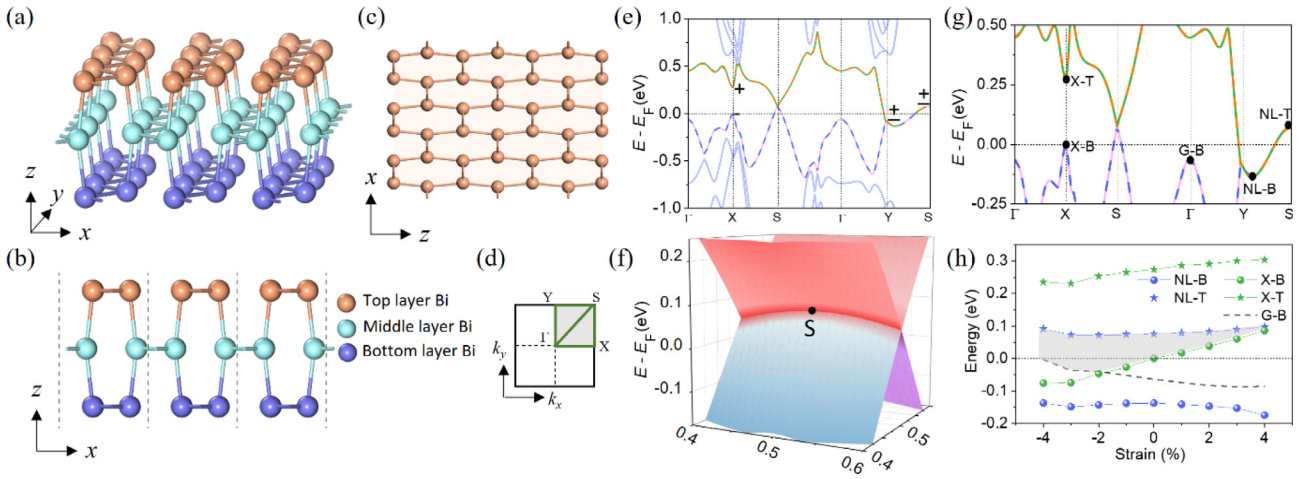

Fig. 1. (Color online) (a) Top and side (b) views of the geometric structure of the 3-AL Bi ("brick phase"). (c) Rotated side view of the geometric structure of a 7-AL Bi, clearly showing its brick-like structure. (d) The first Brillouin zone of 3-AL Bi along with five high-symmetry paths marked in green solid lines. (e) Band structures 3-AL Bi with SOC. Signs "+" and "–" represent the parities of symmetries, respectively. The pink and blue (green and orange) dashed lines represent the two spin components, respectively, while other bands were plotted in the light-blue color for simplicity. (f) Three-dimensional diagram of the linear Dirac nodal-line state of 3-AL Bi with SOC around the S point. (g) Definitions of the lowest (NL-B) and highest (NL-T) energy of the Dirac nodal line, VBM (X-B) and CBM (X-T) at the X point and VBM (G-B) at the Γ point. (h) Variations of the energies of NL-B (blue circle), NL-T (blue star), X-B (green circle), X-T (green star) and G-B (gray dashed line) when applying compressive or tensile uniaxial strains along the *x* direction. The gray shaded area represents the energy windows where the "neat" Dirac nodal line remains.

the square of the combination of $\{C_{2x} \mid (0, ½, 0)\}$ and **IT** equals to −1, namely $[\{C_{2x}$ **IT**$\mid (0, ½, 0)\}]^2 = -1$ is true for all k_x points in line (k_x, π, 0) of the BZ (Fig. 1d). These two relations ensure that the fourfold degeneracy along line (k_x, π, 0) is stable even if strong SOC is present (the Supplementary materials-Methods II). Our group theory derivation proves that the dispersion relations are linear in the k_y direction at the vicinity of the (k_x, π, 0) line (the Supplementary materials-Methods III). These results indicate that the Y-S line is a fourfold degenerated nodal line of the Dirac type, the formation of which is independent of specific orbitals and does not require band inversion.

The fourfold degeneracy of the Y-S nodal line persists under SOC, as shown in the band structures considering SOC (Fig. 1e), which is protected by the $\{C_{2x}\mid (0, ½, 0)\}$, $\{M_y\mid (0, ½, 0)\}$ and **IT** symmetry operations. The strong SOC of Bi opens a 280 meV gap at the X point, which leads to nontrivial edge states at the boundary of 3-AL Bi (Fig. S3 online). The SOC also suppresses the dispersion of the nodal line, where the energy width of the DNL reduces from 0.40 to 0.22 eV (Fig. S2a online). Both the gap opened at X and the narrowed bandwidth of DNL resulted from SOC substantially stand out the DNL states around E_F where the DNL states solely exist from 0.00 to 0.08 eV. A formula cell of the 3-AL Bi contains 30 valence electrons, which are divisible by 2 but not by 4 (the 4*n* + 2 case). This valence electron configuration leads to the fourfold degenerate Dirac bands half-filled that ensures the DNL passes through E_F. Addition or removal of one more electron per atom shifts the nodal line upward or downward from the E_F and the Dirac states are fully filled with 4*n* valence electrons. A 3D plot of the DNL around the S point (Fig. 1f) is used to more clearly illustrate the DNL states. This neat Dirac-line shows a constant density of states in the energy window that a gap is opened at the X point. This unique features result in the anisotropic electron transport and topological properties, e.g., potential long-range Coulomb interaction and flat Landau levels [10,13], much easier to be experimentally measured or tuned. In the band structures calculated using the HSE06 functional (Fig. S4 online), we also observed the SOC resistant fourfold degeneracy, which is not surprising that the fractional translation essentially yields a 4-dimensional irreducible projective Rep to protect the quadruple degeneracy. In other words, the nonsymmorphic symmetry we found guarantees the fourfold DNL under SOC regardless the functional used, the value of lattice constant and the presence of band inversion, while the last is usually required by symmorphic symmetry-protected DNL semimetals [14].

While in-plane strain commonly exists in vdW heterostructures, it is thus of interest to examine how the in-plane strain affects this "neat" DNL property, i.e., the electronic bandgap at the X point and the DNL solely available near E_F (Fig. 1g). Fig. 1h depicts the tendency of the DNL bandwidth (energy difference between NL-B and NL-T, see Fig. 1g) in line Y-S and the energy positions of CBM and VBM at the X point under uniaxial strain applied in the *x* direction. The bandgap was slightly decreased under the strain from –3% to 4%. When the compression strain reaches –2%, the energy window showing the "neat" Dirac nodal line is the largest. In addition to in-plane strain, contact with a substrate or capping layer, sometimes, breaks structural symmetries. The breaking space inversion symmetry causes a gap in the DNL regardless of the inclusion of SOC (Fig. S5a, b online). If the SOC effect is significant, the anti-commutation relation between $\{M_y \mid (0, ½, 0)\}$ and $\{C_{2x} \mid (0, ½, 0)\}$ is required to protect the orbital degeneracy. Breakdown in either of these symmetries reduces the quadruple degeneracy into two double degeneracies, except for high symmetry points Y and S (Fig. S5d online).

The 3-AL Bi layer is not the only material showing the specific $\mathscr{C}_{2v} \times Z_2^T$ symmetry. A 1-AL (Fig. 2a and b), a 5-AL Bi layer (Fig. 2c and d) and the P, As, and Sb analogues of 3-AL Bi all share the same $\mathscr{C}_{2v} \times Z_2^T$ symmetry. Each of those layers was expected a fourfold degenerated DNL semimetal state resistant to strong SOC, which are indeed observable in our calculations (Fig. 2g–i and Fig. S2b, c online), but the electronic states at point X and/or in line Γ–Y strongly interfere with the DNL states. Thus, the 3-AL Bi appears to be the most "neat" platform for studying exotic properties purely induced by the DNL states among all these candidates.

The increased number of layers in those analogues reinforces the thermal stability of each considered element (Fig. 2e). Phonon dispersion spectrum calculations were performed to further verify the dynamic stability of those layers. Though 1AL P/As/Sb/Bi show imaginary frequencies off the Γ point (Fig. S6 online), a substrate

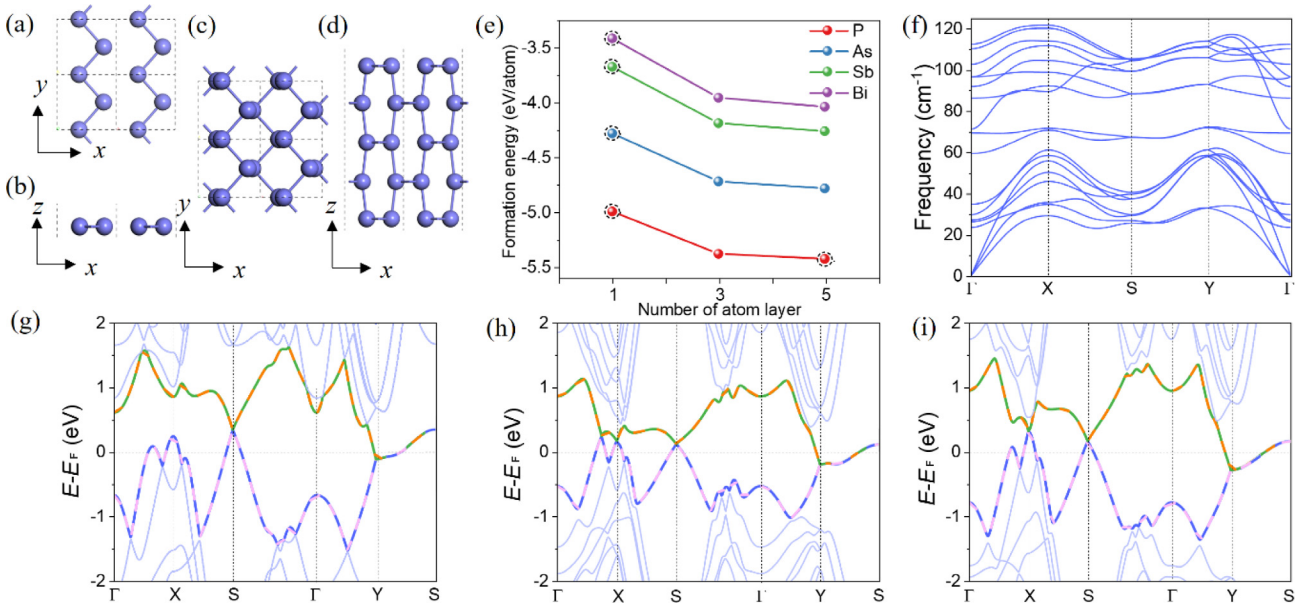

Fig. 2. (Color online) Top (a, c) and side (b, d) views of the geometric structures of mono- (a, b) and five- (c, d) atomic-layer Bi. (e) Relationship between formation energy and atomic layer thickness in P, As, Sb, Bi element. Black dotted circles indicate the presence of imaginary frequencies in phonon spectrum. (f) Phonon spectrum of the 3AL Bi brick layer. Electronic band structures (with SOC) of 3-AL phosphorus (g), arsenic (h), and antimony (i) layers along the same high-symmetric paths and the same color code adopted in Fig. 1d.

could maintain their dynamic stability and impose their nonsymmorphic-symmetry potential fields onto the substrate surface [15]. Thicker layers, except 5AL P (Fig. 2f and Figs. S6, S7 online), exhibit no imaginary frequencies along the paths connecting all high-symmetry points in the BZ, which thus indicates the dynamic stability of this materials category.

In summary, we found that the nonsymmorphic layer group pmma, containing the $\mathscr{C}_{2v} \times Z_2^T$ little co-group, guarantees the formation of 2D DNL semimetals regardless the presence of SOC. This symmetry is imposed into a novel allotrope (the brick phase) of group VA elemental (Bi, Sb, As, and P) layers, and was theoretically predicted to offer robust and fourfold degenerated 2D DNL semimetal states against SOC in line (k_x, π, 0). Intriguingly, the DNL band in every considered layer resides across E_F while other bands are, at least partially, away from it, especially in 3-AL Bi, which results in a "neat" DNL band around the Fermi level. We expect more fascinating properties to be discovered in the heterojunctions and/or alloys of the brick phase layers. The **IT** operation is not a symmetry element of magnetic moments in BZs of ferromagnetic materials, but it does be in anti-ferromagnetic layers. This means that SOC-resistant DNL could also be found in 2D antiferromagnetic materials, whose long-range magnetism and the consequent symmetries as well as electronic structures could be tuned by a magnetic field. In terms of 2D ferromagnetic materials imposing the $\mathscr{C}_{2v} \times Z_2^T$ symmetry, they are considered as candidates for Weyl-point or Weyl-line semimetals. This work, thus, introduces a perspective for the exploration of magnetic DNL semimetals. More importantly, the nonsymmorphic symmetry protection of DNL semimetals can be generalized to other systems, such as phonon, photonic, or magnon bands. This generalization could boost the artificial design and data mining of 2D DNL materials, as well as invite subsequent exploration of their unique physical properties via device measurements.

Conflict of interest

The authors declare that they have no conflict of interest.

Acknowledgments

We gratefully acknowledge financial support from the Ministry of Science and Technology (MOST) of China (2018YFE0202700, 2017YFA0302903, and 2019YFA0308603), the National Natural Science Foundation of China (11622437, 61674171, 61761166009, 11574392, 11974421, 11974422, 11774422, 12174443, and 12134020), the Strategic Priority Research Program of Chinese Academy of Sciences (XDB30000000), the Fundamental Research Funds for the Central Universities, and the Research Funds of Renmin University of China (22XNKJ30 (W.J.) and 21XNH090 (D.P.G.)).

Author contributions

Wei Ji conceived this project. Pengjie Guo, Zheng-Xin Liu, Kai Liu, and Zhongyi Lu performed the symmetry analysis. Deping Guo and Wei Ji performed the first principle calculations. Min Feng and Limin Cao inspired this work with their preliminary experimental results. Min Feng, Limin Cao, together with Shijing Tan, participated in data analysis and discussion. Deping Guo, Pengjie Guo, Zheng-Xin Liu, and Wei Ji wrote the manuscript with inputs from the all authors.

Appendix A. Supplementary materials

Supplementary materials to this short communication can be found online at https://doi.org/10.1016/j.scib.2022.09.008.

References

[1] Fang C, Weng H, Dai X, et al. Topological nodal line semimetals. Chin Phys B 2016;25:117106.
[2] Armitage NP, Mele EJ, Vishwanath A. Weyl and Dirac semimetals in three-dimensional solids. Rev Mod Phys 2018;90:015001.
[3] Wehling TO, Black-Schaffer AM, Balatsky AV. Dirac materials. Adv Phys 2014;63:1–76.
[4] Muñoz-Segovia D, Cortijo A. Many-body effects in nodal-line semimetals: correction to the optical conductivity. Phys Rev B 2020;101:205102.

[5] Shao Y, Rudenko AN, Hu J, et al. Electronic correlations in nodal-line semimetals. Nat Phys 2020;16:636–41.
[6] Fang C, Chen Y, Kee H-Y, et al. Topological nodal line semimetals with and without spin-orbital coupling. Phys Rev B 2015;92:081201.
[7] Wang S-S, Liu Y, Yu Z-M, et al. Hourglass Dirac chain metal in rhenium dioxide. Nat Commun 2017;8:1–7.
[8] Wang Y, Qian Y, Yang M, et al. Spectroscopic evidence for the realization of a genuine topological nodal-line semimetal in LaSbTe. Phys Rev B 2021;103:125131.
[9] Young SM, Kane CL. Dirac semimetals in two dimensions. Phys Rev Lett 2015;115:126803.
[10] Feng B, Fu B, Kasamatsu S, et al. Experimental realization of two-dimensional Dirac nodal line fermions in monolayer Cu_2Si. Nat Commun 2017;8:1–6.
[11] Gao L, Sun JT, Lu JC, et al. Epitaxial growth of honeycomb monolayer CuSe with Dirac nodal line fermions. Adv Mater 2018;30:1707055.
[12] Kowalczyk PJ, Brown SA, Maerkl T, et al. Realization of symmetry-enforced two-dimensional Dirac fermions in nonsymmorphic alpha-bismuthene. ACS Nano 2020;14:1888–94.
[13] Wang C, Zhang Z, Zhou L, et al. Diabolical touching point in the magnetic energy levels of topological nodal-line metals. Phys Rev B 2022;105:045141.
[14] Bernevig A, Weng H, Fang Z, et al. Recent progress in the study of topological semimetals. J Phys Soc Jpn 2018;87:041001.
[15] Tian M, Wang J, Liu X, et al. Creation of the Dirac nodal line by extrinsic symmetry engineering. Nano Lett 2020;20:2157–62.

Deping Guo is pursuing a doctor degree at Department of Physics, Renmin University of China. Her research interest is electronic and magnetic properties of two dimensional layered materials, manipulation of 2D materials through strain or charge doping, and seeking novel 2-dimensional materials.

Pengjie Guo received a Ph.D. degree in Condensed Matter Physics in 2020 from Renmin University of China. He is now a postdoctor of Songshan Lake Materials Laboratory. His research field is computational condensed matter physics, mainly focusing on the topological properties of non-magnetic and magnetic materials.

Zheng-Xin Liu acquired his Ph.D. degree in the Hong Kong University of Science and Technology in 2010 and now he is a professor at the Department of Physics, Renmin University of China. His research interest includes quantum magnetism, magnetic semimetals, superconductors, topological order and topological quantum computation, etc. Recently, he systematically studied the projective representations of anti-unitary groups and then efficiently constructed the k.p theory for itinerant electrons in magnetic systems.

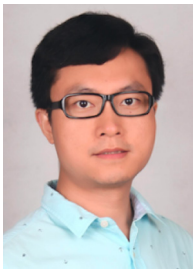

Kai Liu received a Ph.D. degree in Condensed Matter Physics in 2008 from the Institute of Physics, Chinese Academy of Sciences (CAS). He is now a professor at Renmin University of China. His research fields are computational condensed matter physics and surface physics, mainly focusing on the electronic structures and the transport properties of superconducting and magnetic materials.

Wei Ji is a professor of Physics at Department of Physics, Renmin University of China. He received his Ph.D. degree from the Institute of Physics, CAS in 2008. Prior to joining Renmin University of China, he spent four years at McGill University as a visiting scholar and then a postdoctoral fellow. His recent research focuses on surface and interface modeling of emerging low-dimensional electronic materials.